Journal of Nepal Geological Society, 2004, Vol. 30 pp. 167–176

Quality of siltstones for concrete aggregate from Nallu Khola area, Kathmandu valley

***Dev Krishna Maharjan and Naresh Kazi Tamrakar**
Central Department of Geology, Tribhuvan University, Kirtipur, Kathmandu, Nepal
*(*Email: dkmaharjn1@hotmail.com)*

ABSTRACT

The siltstones of the Tistung Formation are the major source of concrete aggregate in the Kathmandu valley. A number of quarries are operating in the valley, especially in the vicinity of the Nallu Khola, for more than three decades. Randomly collected siltstone samples from both banks of the Nallu Khola were studied to reveal their petrography and chemical composition. Crushed rock fragments were investigated to determine their overall aggregate properties. Tests were carried out to determine shape, flakiness index, elongation index, degree of induration, Schmidt hammer value, dry density, water absorption value, aggregate crushing value, and aggregate impact value. The test results indicate that the aggregates are physically, mechanically, and chemically sound.

INTRODUCTION

Several stone quarries are in operation in the Kathmandu valley for more than three decades. They are concentrated mainly in the Halchok, Sitapaila, and Nallu Khola (Tikabhairav) areas (Fig. 1). The Cambrian rocks of the Tistung Formation (Stöcklin 1980) are well distributed in the vicinity of the Nallu Khola, in the southern part of the Kathmandu valley (Fig. 1). Among siltstones, sandstones, and shales characterising the Tistung Formation, the siltstones predominate in the Nallu Khola area. The aggregates produced are supplied to the urban areas without any technical specifications. Hence, this study aims at evaluating the suitability of siltstones for concrete aggregates based on their rock mass characteristics, petrographic study, physical and chemical durability, and mechanical properties.

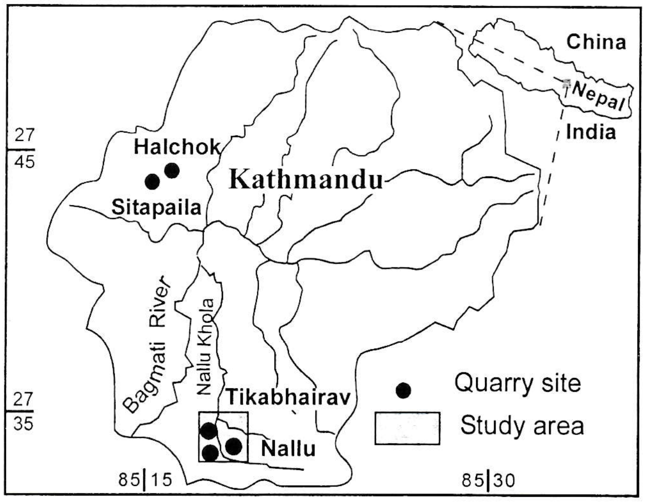

Fig. 1: Maps showing Location of study area

GEOLOGICAL SETTING

The Nallu Khola flows northwards and confluences with the Lele Khola giving rise to the Nakhu Khola (Fig. 2). A thick sequence of the Tistung Formation crops out on both banks of the Nallu Khola and on the uphill side of the road between Tikabhairav and Nayagaun (SE of the study area). Generally, beds strike NW–SE and dip 40°NE. In the middle part of the Nallu Khola area, beds are folded and plunge due northwest. Vertical faults trending NW–SE and a few lineaments are also reported from the Nallu Khola area (Stöcklin and Bhattarai 1977).

The Tistung Formation consists of medium- to thick-bedded, platy to blocky, and light bluish grey siltstone with thin intercalations of sandstone and shale. Rhythmic clastic sequences are observed in the lower, middle, and upper parts of the formation. In the southern region of the study area (locations 1, 2, 3, 4; Fig. 2), the siltstones are medium- to thick-bedded, laminated, and light grey. At location 6, strata show fining-upward sequences, and dip north-westward with an amount less than 45°. They are moderately to slightly weathered, medium- to thick-bedded, and light grey (Fig. 3a). They often contain joints with plumose structures. At locations 9, 10, 11, and 12, strata extend to NE–SW and dip 30° due NW. The exposure comprises thin- to medium-bedded, light grey siltstone (Fig. 3b).

In the middle part of the study area, at locations 13, 14, 15, and 16 (Fig. 2), the siltstones are slabby to massive, medium- to thick-bedded, laminated, and light grey. At present, the left bank of the Nallu Khola is being mined (Fig. 3c, 3d). At Sikharwa (locations 17, 18, and 19; Fig. 2), the strata strike NE–SW and dip 30–60° due NW. They are thin- to medium-bedded, moderately weathered, laminated, and light grey.

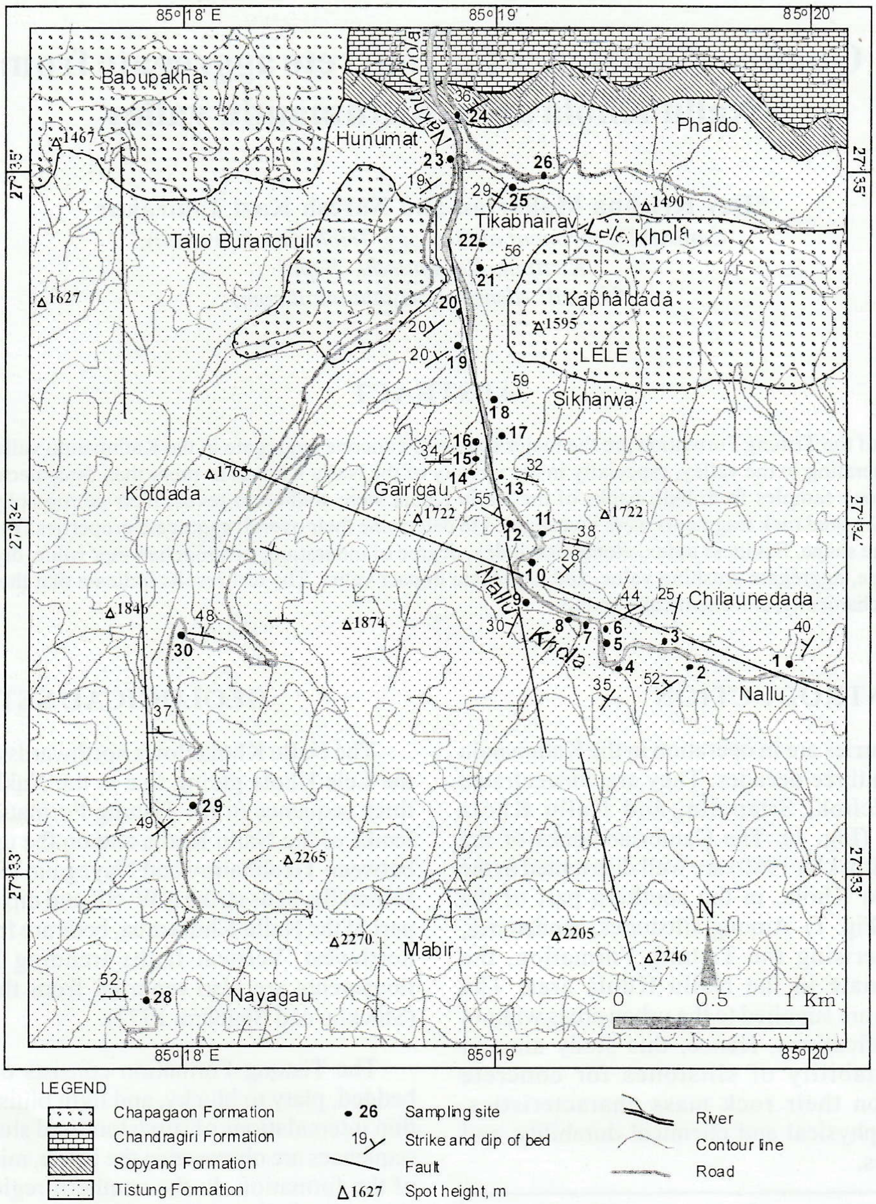

Fig. 2: Geological map with sampling sites (Geology: modified from Stöcklin and Bhattarai 1977)

In the northern part, at Tikabhairav (localities 20, 21 and 22), strata are well exposed on both banks of the Nallu Khola. The siltstones exposed there are medium- to thick-bedded, slabby to blocky, and light grey (Fig. 3c). They contain oscillation ripple marks and exhibit fining-upward gradation. At locations 23, 24, 25 and 26, strata dip northwards at 30–40°. Siltstones therein are slightly weathered, medium bedded, and light grey.

On the right bank of the Nakhu Khola, about 150 m downstream from the bridge, a transitional contact between the Tistung and overlying Sopyang Formations is observed. The Sopyang Formation contains thinly bedded and laminated dark grey calcareous slates.

At Tikabhairav, Kaphaldanda, and Babupakha, fluvial deposits (i.e., the Chapagaon Formation) cover the rocks of the Tistung Formation. These deposits comprise poorly sorted silty-sandy gravel, mud, and muddy sand.

METHODOLOGY

The study area was surveyed on a scale of 1:25,000 to collect information on geological structure, lithology, and rock mass. Representative block samples (1×10^{-3} m^3) as well as fragmented pieces (about 2 kg) were collected from 27 locations in the Nallu Khola area. The investigation of mineralogical and textural properties of rocks was carried

Fig. 3: Outcrops of rocks exposed in the banks and hill slopes of the Nallu Khola

out by studying the thin sections under the polarising microscope. From the block samples, separate cores were obtained for determining their physical properties and durability measures. The fragmented samples were utilised in determining durability measures, shape parameters using axial ratios as well as petrographic image analysis, aggregate crushing value, and aggregate impact value. The data obtained from the petrographic study, physical and stiffness tests, and durability tests were used to evaluate the siltstones.

ROCK MASS CHARACTERISTICS

The rocks of the Tistung Formation contain two to four sets of joints (Table 1). In the southern part of the study area, three sets are found. The southeast-dipping joints predominate in these outcrops. In the middle region, the siltstones contain four sets of joints and most of them dip towards SW. The siltstones located in the northern part contain only two sets of diagonal joints. Joint spacing varies from 5 to 30 cm (moderate spacing) or 0.3 to 1 m (wide spacing). Joints have a wide spacing in the siltstones at locations 3, 4, 24 and 25, but have a moderate spacing in other areas.

Most of the discontinuities are persistent. Their roughness values lie within the range of 6 and 12 on the roughness scale of Barton and Choubey (1977). Their roughness angle frequently ranges from 2° to 4°. The apertures of discontinuities range from 0.1 to 1 mm and they are often filled up with clay. The rock outcrops are faintly to slightly weathered according to the weathering classification of the Geological Society of London (1970). Persistent and closely-spaced joints with wide openings give rise to the fragile rock mass, but highly-spaced joints result in massive rocks.

THIN SECTION STUDY

Twenty-seven rock specimens were classified using the Munsell colour chart (Anon 1991). Their colour was defined in terms of hue, value, and chroma. Thin sections were prepared from 27 rock specimens and were stained for K-feldspar applying Chayes method (Chayes 1952), and for

Table 1: Rockmass characteristics along the Nallu Khola area

Sample	Weathering grade[1]	Seepage	Disconti-nuities	Dip direction/ amount	Persistancy	Spacing, m	Width, mm	Roughness[2]	Roughness angle	Infilling material	Slope direction/amount
1	IA	no	Bedding	300/40°	Continuous	0.05-0.30	1-5	6-8	1°	Clay+vegetation.	170°/50°
			Joint J1	60/39°	Few-cont.	0.05-0.30	0.1-1	8-10	2°	Clay+vegetation	
			Joint J2	171/25°	Few-cont.	0.05-0.30	0.1-1	6-8	1°	Clay+vegetation	
2	II	no	Bedding	318/29°	Continuous	0.05-0.30	1-5	8-10	2°	Mud +vegetation	186°/58°
			Joint J1	265/71°	Discontinuous	0.05-0.30	1-5	10-12	3°	Mud+vegetation.	
			Joint J2	140/67°	Discontinuous	0.05-0.30	0.1-1	8-10	1°	Clay+vegetation	
			Joint J3	110/63°	Discontinuous	0.05-0.30	0.1-1	6-8	2°	Clay+vegetation	
3	IB	no	Bedding	300/40°	Continuous	0.30-1.00	1-5	10-12	8°	Clay+vegetation.	177°/48°
			Joint J1	60/39°	Continuous	0.30-1.00	1-5	6-8	3°	Clay+vegetation.	
			Joint J2	171/25°	Few-cont.	0.30-1.00	0.1-1	8-10	3°	Clay+vegetation	
			Joint J3		Few-cont.	0.30-1.00	0.1-1	8-10	3°	Clay+vegetation	
4	IB	no	Bedding	318/29°	Continuous	0.30-1.00	1-5	6-8	1°	Clay+vegetation.	180°/30°
			Joint J1	265/71°	Continuous	0.05-0.30	0.1-1	8-10	2°	Mud+vegetation	
9	II	no	Bedding	33/32°	Continuous	0.05-0.30	1-5	10-12	3°	Mud+vegetation	210°/68°
			Joint J1	206/60°	Continuous	0.05-0.30	1-5	14-16	7°	Mud+vegetation	
			Joint J2	285/76°	Few-cont.	0.05-0.30	0.1-1	14-16	6°	Clay+vegetation	
			Joint J3	320/55°	Discontinuous	0.05-0.30	0.1-1	6-8	1°	Clay+vegetation.	
10	IB	no	Bedding	290/28°	Continuous	0.05-0.30	0.1-1	10-12	4°	Mud+vegetation.	260°/65°
			Joint J1	130/60°	Few-cont.	0.30-1.00	0.1-1	8-10	1°	Mud+vegetation.	
11	IB	no	Bedding	355/50°	Continuous	0.05-0.30	1-5	6-8	1°	Clay+vegetation	269°/71°
			Joint J1	195/90°	Few-cont.	0.30-1.00	0.1-1	8-10	1°	Clay+vegetation	
			Jont J2	205/55°	non-cont.	0.05-0.30	<0.1	10-12	4°	No	
15	IB	no	Bedding	8/34°	Continuous	0.05-0.30	1-5	8-10	3°	Clay+vegetation	160°/60°
			Joint J1	187/34°	Few-cont.	0.05-0.30	0.1-1	8-10	3°	Clay+vegetation	
			Joint J2	120/56°	Few-cont.	0.05-0.30	0.1-1	10-12	4°	Clay+air	
18	IB	no	Bedding	340/59°	Continuous	0.05-0.30	1-5	8-10	3°	Clay+vegetation	185°/55°
			Joint J1	Vertical	Discontinuous	0.05-0.30	<0.1	8-10	1°	Clay	
			Joint J2	260/85°	Discontinuous	0.05-0.30	0.1-1	8-10	2°	Clay+vegetation	
			Joint J3	160/33°	Few-cont.	0.05-0.30	0.1-1	10-12	4°	Clay	
			Joint J4	220/60°	Few-cont.	0.05-0.30	0.1-1	10-12	4°	Clay	

[1]Geological Society of London, 1970, IA-Fresh, IB-Faintly weathered, II-Slightly weathered; [2]Barton and Choubey, 1977, Typical roughness profiles

Table 2: Results of analysis of thin sections of siltstone

Sample number	Colour (hue/ value/ chroma)		Micro-structure	Texture	Composition, %						
					Quartz	Feldspar	Mica	Heavies	Unidentified	Cement	Void
1	5B 6/1	Light bluish grey	Massive	Medium silt	73	1	7	-	3	16	-
2	5B 6/1	Light bluish grey	Massive	Coarse silt	78	-	7	-	4	11	-
3	5B 6/1	Light bluish grey	Massive	Medium silt	70	3	18	-	-	9	-
4	5B 7/1	Light bluish grey	Less foliated	Medium silt	79	2	6	3	-	10	-
5	5B 6/1	Light bluish grey	Less foliated	Fine Silt	78	1	6	2	-	13	-
6	5B 6/1	Light bluish grey	Less foliated	Medium silt	65	1	22	3	3	6	-
7	5B 6/1	Light bluish grey	Massive	Coarse silt	68	1	18	2	-	9	2
8	5B 6/1	Light bluish grey	Well foliated	Coarse silt	85	2	4	2	2	5	-
9	5B 6/1	Light bluish grey	Well foliated	Fine silt	81	1	10	3	-	3	2
10	5B 6/1	Light bluish grey	Massive	Coarse silt	73	1	20	2	1	3	-
11	5B 6/1	Light bluish grey	Massive	Coarse silt	76	1	5	2	5	11	-
12	5B 6/1	Light bluish grey	Massive	Coarse silt	56	-	22	1	4	17	-
15	5B 6/1	Light bluish grey	Massive	Coarse silt	59	2	23	1	-	15	-
17	5YR 6/2	Pale brown	Less foliated	Fine silt	82	1	3	2	5	2	5
18	5B 6/1	Light bluish grey	Well foliated	Coarse silt	83	1	7	4	2	1	2
19	5Y 7/2	Yellowish grey	Massive	Coarse silt	65	-	15	2	1	2	15
20	5B 7/1	Light bluish grey	Massive	Coarse silt	80	1	8	2	2	5	2
21	5Y 8/1	Yellowish grey	Foliated	Coarse silt	78	1	12	1	2	5	1
22	10YR 7/2	Pale yellowish brown	Massive	Coarse silt	55	-	25	5	5	10	-
23	10YR 8/4	Greyish orange	Massive	Fine silt	65	2	8	17	-	8	-
24	5B 7/1	Light bluish grey	Massive	Medium silt	50	-	21	12	-	17	-
25	5B 7/1	Light bluish grey	Less foliated	Coarse silt	82	-	8	2	-	7	1
26	10YR 7/2	Pale yellowish brown	Less foliated	Coarse silt	81	-	6	2	4	5	2
27	5YR 7/1	Light brownish grey	Less foliated	Coarse silt	65	4	10	11	-	10	-
28	10YR 7/2	Pale yellowish brown	Less foliated	Fine silt	72	1	7	11	2	7	-
29	5YR 7/1	Light brownish grey	Less foliated	Fine silt	65	3	6	12	-	14	-
30	10YR 7/2	Pale yellowish brown	Less foliated	Coarse silt	80	1	5	8	-	6	-

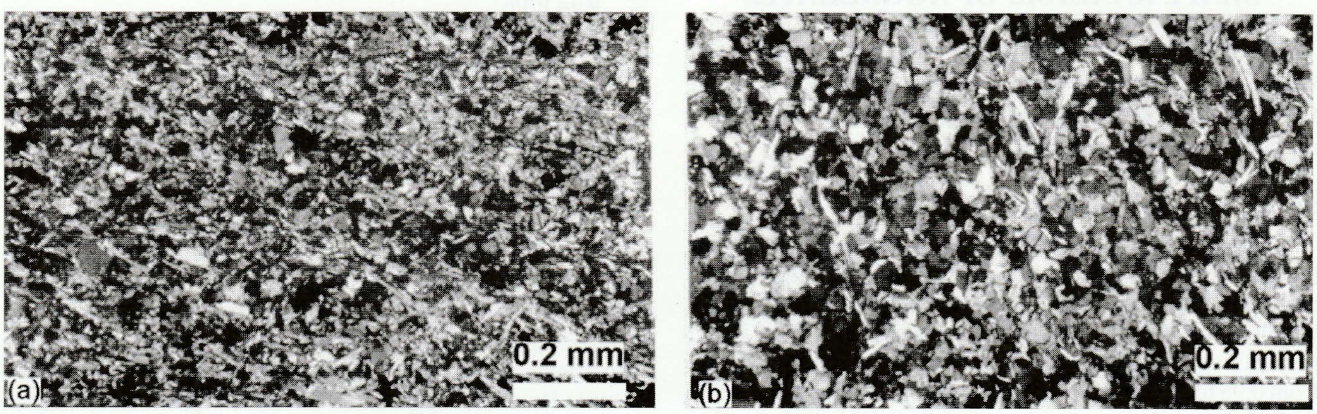

Fig. 4: Photomicrographs of siltstone; (a) Interlocked and elongate quartz grains and micas (location 9) and (b) interlocked quartz grains (Location 15)

swelling clay mineral (smectite) using methylene blue. Composition of rocks was determined following the point-counting method of Blackburn and Dennen (1988). Their colour, microstructure, texture, and composition are listed in Table 2.

Most of the light bluish grey specimens are fresh. Some samples show pale yellowish brown and light brownish grey colours resulted due to ferruginous cements and a few altered grains. Siltstones are frequently massive to well-foliated (Fig. 4a) and sporadically less foliated (Fig 4b). Their grain size varies from fine to coarse silt.

Quartz is the dominant mineral in all the samples, whereas feldspar, mica, and heavy minerals constitute a minor proportion. In some samples, micas (mainly muscovite) represent around 20%, where fresh authigenic muscovite displays sharp boundaries. The rock is normally free of voids and cemented mostly by authigenic silica with sporadic argillaceous and ferruginous material. Generally, subrounded quartz grains are interlocked. In some sections, elongated quartz grains are aligned parallel to the foliation.

Most of the rocks are slightly foliated. Samples 8, 9, and 18 are well foliated, in which quartz- and mica-rich bands can be distinguished. A high proportion of quartz with strong siliceous cement and interlocked grains make the siltstones indurated.

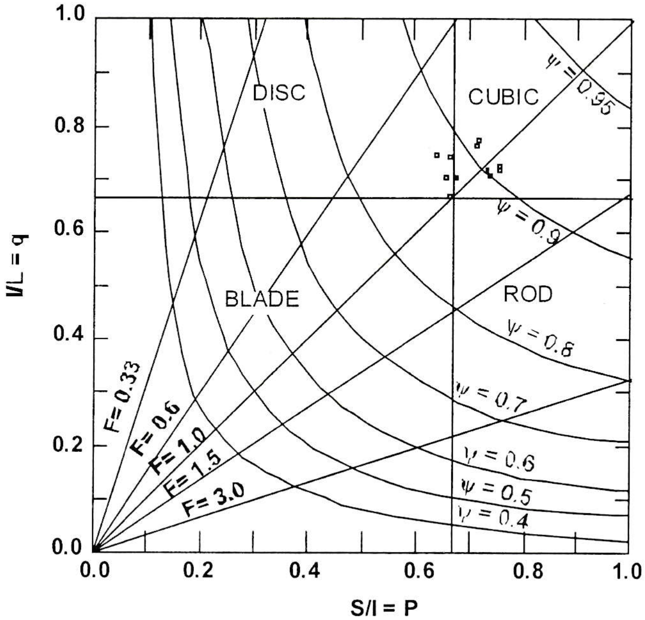

Fig. 5: Shape diagram indicating mean forms of aggregate samples

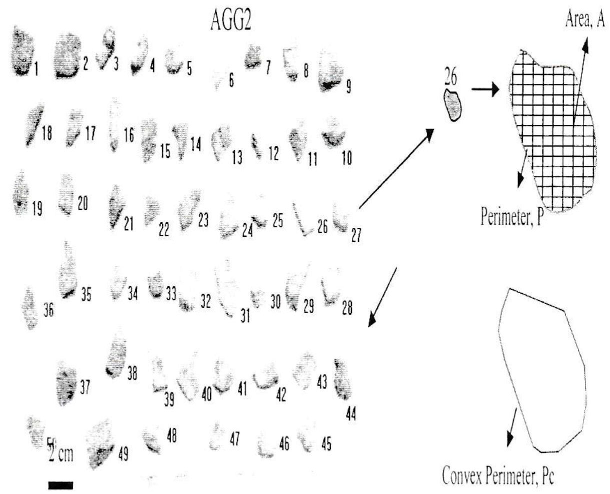

Fig. 6: Determination of perimeter and area of a grain. Sample 26 shown as an example.

SHAPE ANALYSIS OF AGGREGATES

The aggregates were studied for their shape factor (F), sphericity (Ψ), roughness index (Ru), roundness index (Rn), flakiness index (FI), and elongation index (EI). The results are summarised in Table 3.

Shape factor and sphericity

Based on the longest (L), intermediate (I), and shortest (S) dimensions of each grain, the shape was quantified in terms of flatness ratio (p = S/I) and elongation ratio (q = I/L), which range from 0.6307 to 0.7491 and 0.6597 to 0.7722, respectively. Shape factor (F) is the ratio q/p, and ranges from 0.95 to 1.18 in most of the samples indicating their cubic to disc shape. However, the plot of flatness and elongation ratios indicates that the aggregate grains are mostly of cubic shape (Fig. 5).

Sphericity was calculated using the flatness and elongation ratios (Janoo 1998) as given below.

$$\psi = \frac{12.8\left(\sqrt[3]{p^2 q}\right)}{1+p(1+q)+6\sqrt{1+p^2\left(1+q^2\right)}}$$

It ranges from 0.863 to 0.926 (Table 3) and shows that the grains possess high sphericity.

Roughness and roundness

Roughness and roundness indices of Janoo (1998) were measured using the computer software NIH Scion Image Analyser and were calculated from the following relations.

Ru= P/Pc

$Rn = 4.\pi.A/P^2.100$

where Ru is roughness index, Rn is roundness index, A is area of particle, P is perimeter, and Pc is convex perimeter (Fig. 6).

For a smooth material, the roughness index equals unity. As the roughness increases, the roughness index also increases. Rough aggregates are desirable because their workability with cement is good (Kaplan 1961; Neville 1996). The roundness index of a perfect circle is 100. As the material becomes angular, the roundness index decreases (Janoo 1998). Rounded aggregates produce significantly higher permanent deformation than angular ones. Rounded particles easily slip whereas angular ones have to overcome higher frictional forces at contact interfaces during compression (Holtz and Kovacs 1981). Internal friction angle increases with increasing angularity and surface roughness (Holtz and Kovacs 1981).

The roughness index of siltstone grains ranges from 1.19 to 1.30, whereas their roundness index varies from 49.77 to 58.62 (Table 3). Most of the aggregate grains show relatively high roughness and moderate roundness.

Flakiness and elongation indices

Flakiness and elongation indices were determined using the methods of determining particle shape by British Standard Institution (1975; 1989). For determining flakiness index (FI) and elongation index (EI), eleven aggregate samples, each with 50 grains were used. For EI, the aggregate

Table 3: Results of shape analyses of aggregates

Sample	Parameters from axial ratio measurement					Parameters from image analysis					BS812	
	p	q	F	Form	Y	P pixel	Pc pixel	A (sq pixel)	Ru	Rn	FI (%)	EI (%)
1	0.67	0.70	1.05	cubic	0.879	70.32	57.26	207067.81	1.23	53.31	16.7	59.6
2	0.66	0.74	1.13	disc	0.891	67.06	52.73	183368.32	1.27	51.91	22.1	83.2
5	0.73	0.72	0.99	cubic	0.911	74.42	62.81	255018.29	1.19	58.62	22.9	68.3
6	0.66	0.66	1.00	disc	0.863	81.02	65.07	266679.22	1.24	51.72	18.9	57.9
9	0.75	0.72	0.95	cubic	0.909	65.91	53.56	181637.40	1.23	53.23	18.8	82.7
10	0.73	0.70	0.96	cubic	0.898	75.90	61.57	225215.04	1.23	49.77	19.5	54.4
11	0.75	0.72	0.97	cubic	0.905	71.53	58.03	202157.86	1.23	50.3	14.5	59.6
17	0.63	0.75	1.18	disc	0.878	75.50	61.21	239727.83	1.23	53.54	17.2	48.8
20	0.71	0.77	1.08	cubic	0.905	75.39	60.88	238449.41	1.24	53.41	15.9	64.0
21	0.71	0.77	1.09	cubic	0.918	70.41	55.14	195682.03	1.30	50.25	11.3	66.9
23	0.65	0.70	1.08	disc	0.926	73.60	60.26	225133.22	1.22	52.91	18.0	40.9

of size 10 to 14 mm was weighed. The aggregate was passed through the length gauge of width 21.6±0.2 mm, such that the greatest grain dimension was aligned along the two pins of the gauge. The fraction, which did not pass through the gauge, was weighed. EI was calculated as

$$EI = \frac{y}{w} \cdot 100\,\%$$

where y is weight of the fraction not passing through the length gauge, and w is the weight of the test sample.

FI was determined using the thickness gauge of length 26.4 mm and width 6.6 mm. For this test, the aggregate sample of size 9.5 to 13.2 mm was weighed. Each aggregate grain was allowed to pass though the thickness gauge. The fraction, which passed through the slot, was weighed. FI was calculated as below:

$$FI = \frac{x}{w} \cdot 100\,\%$$

where x is weight of the fraction passing through the thickness gauge, and w is the weight of the test sample.

A low percentage of FI shows that the aggregates contain only a few flat grains. The high percentage of EI indicates the presence of a small number of elongated grains. In the studied samples, FI ranges from 14 to 22% and EI varies from 40.87 to 83.17% (Table 3) indicating that there are not many flat or elongated grains.

DRY DENSITY AND WATER ABSORPTION VALUE

The physical properties of aggregate, such as dry density (ρ_{dry}) and water absorption value (WAV), were measured. Dry density and WAV were determined for cylindrical samples according to calliper and saturation method (ISRM 1979).

The dry density of samples ranges from 2126 kg/m^3 to 2745 kg/m^3 with an average value of 2585 kg/m^3. Most samples bear less than 1% WAV (Table 4), thus showing very low effective porosity. Only few siltstones from the north of the study area contain WAV between 1.0 and 6.6 %. The dry density values indicate that the siltstones are much denser than lightweight aggregates. Low WAV indicates low accessibility for water to pass through the intact rock.

Stiffness

Stiffness of aggregate grains was evaluated based on Schmidt hammer test, induration, aggregate crushing value (ACV), and aggregate impact value (AIV).

Schmidt hammer test

Schmidt rebound hammer test was carried out in in-situ siltstones using an L-type hammer. Out of 20 observations, the higher 10 values were averaged and taken as the Schmidt hammer value (SHV), which ranges from 32 to 56 (Table 4). The SHVs were used along with the density of samples to derive the unconfined compressive strength (UCS) according to Deere and Miller (1966). The UCS ranges from 45 to 180 MPa, which indicates that the siltstones belong to medium- to high-strength rocks.

Induration

Induration indicates the degree of freshness or stiffness of rock or rock material. The induration of intact rock specimen was measured following Larsen et al. (1995). Most of the samples fall on H4 (i.e., strongly indurated) and H5 (i.e., very strongly indurated), and a few on H3 (i.e., indurated) categories. The strongly to very strongly indurated samples are compact and well interlocked.

Crushing and impact values

Aggregate crushing value (ACV) and aggregate impact value (AIV) were determined using a compression testing machine and a hammer, respectively following ASTM (1979). ACV provides a relative measure of resistance to crushing under a gradually applied compressive load. To achieve a good quality of aggregate, low ACV is preferred (ASTM 1979). ACV was obtained using the equation:

$$ACV = \frac{W2}{W1} x100\%$$

where W1 = total weight of test sample (g) and W2 = weight of aggregate passing 4.75 mm sieve after the test (g).

The ACV of siltstones ranges from 22.13 to 31.96% (Table 4). It is satisfactory for using as the concrete aggregate, but the desirable value is <16% for road pavement design.

AIV was calculated using the following equation:

$$AIV = \frac{W3}{W1} x100\%$$

where W1 = weight of original sample and W3 = weight of the fraction after the test, passing through 2.36 sieve.

Hobbs (1964) related AIV with compressive strength to classify rocks with respect to their toughness. The AIV of siltstones ranges from 13.75 to 19.5%, which belongs to the desirable range (10–20%) according to ASTM (1979). This range also indicates that all the aggregates tested are strong (Hobbs 1964) and are resistant to impact. Therefore, these are suitable for pavements.

DURABILITY

To evaluate chemical and mechanical durability of aggregates against weathering, ethylene glycol soak test, methylene blue absorption test, and magnesium sulphate soundness test were performed.

Ethylene glycol soak test

Ethylene glycol causes rapid expansion of swelling clays by penetrating into their lattice. The core samples were immersed in ethylene glycol for 30 days. Then, a degree of disintegration and time required to approach the worst

Table 4: Physical properties, stiffness measures and durability of siltstone

Sample	Physical properties		Stiffness measures					Durability measures		
	WAV %	Dry density Kg/m³	SHV	UCS[1] Mpa	Induration[2]	ACV %	AIV %	STI	MBAV %	MSV %
1	0.71	2550	48	125	H4	23.3	14.9	1	< 1%	0.25
2	0.22	2683	47	113	H4	23.4	13.8	1	< 1%	13.6
3	0.40	2740	48	125	H3	23.1	15.0	1	< 1%	-
4	0.40	2607	47	113	H4	23.8	15.4	1	< 1%	-
5	0.19	2253	48	125	H3	22.1	15.0	1	< 1%	13
6	0.31	2679	50	140	H4	22.7	14.3	1	< 1%	0.4
7	0.17	2700	46	100	H4	24.2	16.3	1	< 1%	-
9	0.57	2664	46	100	H4	22.5	13.8	1	< 1%	2.06
10	0.52	2711	49	132	H3	23.0	14.7	1	< 1%	0.47
11	0.30	2657	51	147	H5	22.7	14.7	1	< 1%	0.33
12	0.20	2744	51	147	H4	22.6	14.6	1	< 1%	-
13	0.63	2745	56	180	H3	21.2	14.7	1	< 1%	-
14	0.20	2739	52	150	H3	23.3	15.5	1	< 1%	-
15	0.22	2749	40	75	H3	25.2	17.0	1	< 1%	-
17	0.18	2493	38	70	H5	25.4	17.2	1	< 1%	0.62
18	0.26	2650	39	73	H4	25.3	17.1	1	< 1%	-
19	2.70	2570	34	56	H3	28.3	19.5	1	< 1%	-
20	1.87	2476	32	50	H4	26.1	18.1	1	< 1%	0.59
21	1.86	2538	29	45	H3	24.7	19.5	1	< 1%	0.48
22	3.37	2451	43	90	H3	25.3	15.0	1	< 1%	-
23	6.60	2126	47	113	H3	23.8	15.4	1	< 1%	0.53
24	1.30	2596	43	90	H3	25.4	15.5	1	< 1%	-
25	0.60	2711	42	85	H4	24.8	16.6	1	< 1%	-
26	1.36	2647	32	50	H4	26.1	18.1	1	< 1%	-
27	1.23	2548	38	70	H5	25.4	17.2	1	< 1%	-
28	2.78	2347	35	58	H4	25.8	17.7	1	< 1%	-
29	0.77	2638	40	75	H5	25.2	17.0	1	< 1%	-
30	2.96	2433	38	70	H4	25.4	17.2	1	< 1%	-

[1]Estimated using chart of Deere and miller (1966); [2]Larsen et al. (1995), H1-Indurated, H4-Strongly indurated, H5-Very strongly indurated

condition were recorded (Haskins and Bell 1995) to obtain the soak test index (STI). The index was equal to 1 for all the samples. It showed that the samples are unaffected by ethylene glycol, which is explained either by a low proportion of swelling clays or their low effective porosity. Therefore, the samples are quite resistant to chemical weathering.

Methylene blue adsorption value (MBAV)

In this test, thin sections of siltstones were treated with methylene blue solution (0.5 g methylene blue + 125 ml distilled water + 125 ml ethanol). The assumption made was that swelling clays are affected by the methylene blue because of cation exchange capacity (Hang and Brindley 1970). A per cent count of area occupied by blue dye in the thin sections (i.e., MBAV) was determined under a polarising microscope. As the value was less than 1%, the samples contain a negligible amount of swelling clays.

Magnesium sulphate value

Magnesium sulphate value (MSV) is the measure of soundness of aggregate. The aggregates of size 10–14 mm and of weight 425 ± 5 g were immersed in the magnesium sulphate solution of density 1.292±0.008 g/ml for 48 hours and were subsequently dried out. The process was repeated for five times. MSV was calculated as below.

$$MSV = \frac{(M1 - M2)}{M1} x100\%$$

where M1=initial mass of the test specimen and M2 = the mass of the specimen retained on 10 mm sieve after the fifth cycle.

An MSV greater than 15% implies frost susceptibility. Since MSV varies from 0.21 to 13.64% in the tested samples, they are frost resistant.

SUITABILITY OF SILTSTONES

Table 5 presents a comparison of the obtained test results with the desired indices. The siltstones from locations 15 to 22 and 24 to 30 possess slightly higher ACV and AIV, lower SHV and UCS, and higher WAV than the rest (i.e., locations 1 to 14, and 23).

The texture of aggregate grains is angular and rough. Their EI is high and FI is low, indicating that the siltstones give rise to a low amount of flat and elongate grains when crushed. The siltstones therefore have good workability with cement.

The siltstones bear less than 4% WAV, indicating very low effective porosity that prevents the solvents from penetrating into them. Dry density of siltstones lies in the intermediate-weight range (between 2000 and 3000 kg/m^3).

Table 5: Evalutation of siltstone the Nallu Khola area

Aggregate property	Desirable value	Obtained value	Remarks
Roundness/roughness	Angular/rough	Angular/rough	Angular with rough surface texture
Form/sphericity	cubic to bladed and high sphericity		
Flakiness index (FI)	Low	14 – 22%	Low amount of flate particles.
Elongation index (EI)	High	40.87-83.17	Low amount of elongate particles
Weathering grade	I to Ib	Ib-II	Rocks are nearly fresh
Induration	H3 to H5 indurated to very strongly indurated	H3-H4	Indurated to strongly indurated rocks
WAV	<1% to 5% (<3% reasonable)	0.20-3.37%	Low effective porosity
Dry density	2000-3000 Kg/m^3	2126-2745 kg/m^3	Medium weight aggregate
UCS	110-221 Mpa (high strength)	45-180 Mpa	Medium to high strength rock
	55-110 Mpa (medium strength)		
ACV	<16% to 25%	22.027-28.3%	Strong rock
AIV	10-20 (strong rock)	13.75-19.5%	Strong rock
STI	1= no obvious effects within 30 days	1	Highly resistant to chemical weathering
	2 = minor spalling of particles between 21 and 30 days		
MBAV	<1%	< 1%	Sound and low amount of swelling clay
MSV	< 15%	0.21-13.64%	Resistant to freeze and thaw

The siltstones are nearly fresh to faintly weathered, as indicated by classes Ib and II in Table 1. They fall between H3 to H5 categories of induration (Table 4). UCS values show that the siltstones are of medium to high strength. ACV and AIV of siltstones also indicate that they are strong rocks.

STI and MSV of the siltstones are 1 and less than 15%, respectively. These parameters indicate that the siltstones are resistant to chemical and mechanical weathering. Similarly, MBAV shows that the swelling clay is present in an insignificant amount, and therefore the rock is also resistant to swelling.

CONCLUSIONS

The siltstones from the Nallu Khola area are faintly to slightly weathered and possess 2 to 4 sets of joints. The siltstones are medium- to coarse-grained, quartz-rich, and their grains are interlocked by siliceous cement. They contain some authigenic micas also. The aggregate grains derived from crushing are almost cubic in shape. They are rough and angular with good workability potential.

The degree of induration, UCS, ACV, and AIV of the grains show that the siltstones are mechanically sound. They belong to medium-weight aggregates. Low WAV, STI, MBAV and MSV of the siltstones indicate that the rock is resistant to frost and chemical weathering. As most of the obtained values from different tests are within the desirable limits, the siltstones are appropriate for concrete aggregates.

ACKNOWLEDGEMENT

We thank Dr P. C. Adhikary, Head, Central Department of Geology, Tribhuvan University, Kirtipur, Kathmandu, Nepal, for providing the laboratory facilities.

REFERENCES

Anon, 1991, *Rock color chart*, Geological Society of America (Munsell color).

ASTM, 1979, *Standard method of test for triaxial compressive strength of undrained rock core specimens without pore pressure measurements.* American Soc. Test. Material, Annual Book of ASTM Standards, 632 p.

Barton, N. and Choubey, V., 1977, The shear of Rock Joints in Theory and Practice, v. 10, pp. 1–54.

Blackburn W. H. and Dennen W. H., 1988, *Principles of mineralogy*, second edition, Wm. C. Brawn Publisher, 443 p.

British Standard Institution, 1975, Methods of determination of particle shape. BS 812, part 1, BSI, London.

British Standard Institution, 1989, Methods of determination of particle shape. BS 812, part 105, BSI, London.

Chayes, F., 1952, Staining of potash feldspars with sodium cobaltinitrite in thin sections, American Minerals, v. 37, pp. 337–390.

Deere, D. U. and Miller, R. P., 1966, Engineering classification and index properties for intact rocks. Tech Rep AFWL-TR Air-force Weapons Laboratory, New Mexico, pp. 65–116.

Geological Society of London, 1970, The logging of rock cores for engineering purposes; Geol. Soc. (London) Eng. Group Working Party, Q. Jour. Engg. Geol., v. 3, pp. 1–24.

Hang, P. T., Brindley, G. W., 1970, Methylene blue adsorption by clay minerals, determination of surface area and cation exchange capacities. Clay Organic Studies XVIII, Clays and Clay Minerals, v. 18, pp. 203–221.

Haskins D. R. and Bell F. G., 1995, Darkensbery basalts; their alteration, breakdown and durability, Quarterly Jour. of Engg. Geol., v. 28, pp. 287–302.

Hobbs D. W., 1964, Rock compressive strength, Coll. Engg., v. 14, pp. 287–292.

Holtz, R. D. and Kovacs, W. D., 1981, *An introduction to Geotechnical engineering*. Eaglewood Cliffs, New Jersey, Prentice-Hall, Inc.

ISRM, 1979, Suggested methods for determining water content, porosity, density, absorption and related properties and swelling and slake-durability index properties: Intl. Soc. Rock mech. Comm. on Standardization of Laboratory and Field Tests, Intl. Jour. Rock Mech. Min. Sci. and Geomech. Abstr., v. 16, pp. 141–156.

Janoo, V. C., 1998, Quantification of Shape, Angularity, and Surface Texture of Base Course Materials, US Army Corps of Engineers, Special Report 98-1, pp. 1–22.

Kaplan, M. F., 1961, Crack propagation and fracture of concrete, Jour. American concrete Institute, v. 58, pp. 591–610.

Larsen, F. J., Villumsen, A., Fredericia, J., Gravesen, P., Fojed, N., Knudsen, B., and Baumann, J., 1995, A Guide to Engineering Geological soil Description, Danish Geotechnical Society, Bulletins.

Neville, A. M., 1996, *Properties of concrete*. Fourth edition, Addison Wesley Longman, Essex, England.

Stöcklin, J., 1980, Geology of Nepal and its regional frame, Jour. Geol. Soc. London, v. 137, pp. 1–34.

Stöcklin, J. and Bhattarai, K. D., 1977, Geology of Kathmandu Area and central Mahabharat Range, Nepal Himalaya. Kathmandu: HMG/UNDP Mineral Exploration Project, Technical Report, New York, 64 p. (Unpublished).